Human Molecular Genetics, 2012, Vol. 21, No. 5 ***1155–1171***
doi:10.1093/hmg/ddr544
Advance Access published on November 21, 2011

The Nek8 protein kinase, mutated in the human cystic kidney disease nephronophthisis, is both activated and degraded during ciliogenesis

Detina Zalli, Richard Bayliss and Andrew M. Fry*

Department of Biochemistry, University of Leicester, Lancaster Road, Leicester LE1 9HN, UK

Received October 17, 2011; Revised and Accepted November 16, 2011

Mutations in the never-in-mitosis A-related kinase, Nek8, are associated with cystic kidney disease in both humans and mice, with Nek8 being the *NPHP9* gene in the human juvenile cystic kidney disease, nephronophthisis. Human Nek8/NPHP9 localizes to centrosomes and the proximal region of cilia in dividing and ciliated cells, respectively. However, the regulation of Nek8 kinase activity, as well as its role in ciliogenesis, remains to be defined. Here, by establishing Nek8 kinase assays, we first demonstrate that the localization of Nek8 to centrosomes and cilia is dependent on both kinase activity and the C-terminal non-catalytic RCC1 domain. The kinase domain alone is active, but does not localize correctly, while the RCC1 domain localizes correctly and can be phosphorylated by Nek8. We propose that centrosome recruitment is mediated by the RCC1 domain, but requires a conformational change in the full-length protein that is promoted by autophosphorylation. Interestingly, three human NPHP9-associated mutants retain full kinase activity. However, only two of these, L330F and A497P, localize correctly, suggesting that the third mutant, H425Y, disrupts a centrosome targeting sequence in the RCC1 domain. Importantly, we find that induction of ciliogenesis upon cell cycle exit is accompanied by both activation and proteasomal degradation of Nek8, and that activation is dependent upon phosphorylation within the catalytic domain. Taken together, these findings reveal important insights into the mechanisms through which Nek8 activity and localization are regulated during ciliogenesis.

INTRODUCTION

Nephronophthisis (NPHP) is a rare, early-onset, cystic kidney disease. It is one type of a wider spectrum of inherited diseases that share many clinical symptoms and are collectively known as ciliopathies. In these diseases, the underlying cellular defect is in the generation, organization or function of a specialized organelle, called the primary cilium. Primary cilia are small hair-like projections present on most cells of the human body. They act as antennae to detect extracellular mechanical and chemical signals that are then transduced via intracellular signalling pathways to give coordinated responses, including proliferation and differentiation (1,2). It is now understood that these responses are crucial to development and homeostasis in multicellular organisms explaining why defects in this structure underlie human ciliopathies (3–5).

Morphologically, the primary cilium, which is largely analogous to the flagella in different biological systems, consists of a plasma membrane extension that surrounds a microtubule axoneme. The axoneme itself is composed of a cylindrical ring of nine microtubule doublets that extend out from the distal end of a basal body that sits at the cytoplasmic surface. The connection between the basal body and the axoneme is known as the transition zone and is the region where proteins enter or exit from the cilium, often trafficked in an active manner by the intraflagellar transport machinery. Basal bodies, being short cylinders of nine microtubule triplets, are analogous in structure to centrioles that are found within the centrosome, the primary microtubule organizing centre of higher eukaryotes. Indeed, basal bodies and centrioles are interchangeable structures; in proliferating cells, the centrioles sit within the centrosome and anchor the

*To whom correspondence should be addressed. Tel: +44 1162297069; Fax: +44 1162297018; Email: amf5@le.ac.uk

pericentriolar material that is required to nucleate microtubules both in interphase and mitosis, while upon exit from the cell cycle and entry into quiescence, the centrioles move to the cell surface and start to act as basal bodies. Here, the older one of the pair, previously the mother centriole, attaches to the membrane via its distal appendages and initiates the growth of the axonemal microtubules directly from its distal end (6).

Ciliopathies are associated with a wide and diverse spectrum of clinical phenotypes that include retinal degeneration, left–right asymmetry defects, polydactyly, anosmia, mental retardation and obesity. However, one of the most common defects seen in most ciliopathies is cystic dilatation of tubules that develop in the kidney as a result of failure to detect flow through the tubules of these organs. Autosomal dominant polycystic kidney disease (ADPKD) is the most common monogenic disorder known to man, with a frequency of 1:400–1:1000. It is caused by mutations in the *PKD1* or *PKD2* genes that encode the primary cilium membrane proteins, polycystin-1 (PC-1) and polycystin-2 (PC-2), respectively (7). Autosomal recessive PKD (ARPKD) on the other hand is rare and results from mutations in the PKHD1 gene that encodes a transmembrane protein, fibrocystin/polyductin, that localizes to the cilium and centrosome in renal epithelial cells.

NPHP represents a distinct autosomal recessive kidney disease that tends to be early onset and is the main genetically defined cause of end-stage renal failure within the first three decades of life (8). Unlike PKD, where an increasing number of large kidney cysts lead to severely enlarged kidneys, NPHP is characterized by tubular basement membrane thickening, tubular atrophy, tubulointerstitial nephritis and, eventually, cyst-like structures at the junction of the cortex and medulla. So far, 11 distinct *NPHP* loci have been identified whose mutation causes this disease, while mutations in at least 7 other genes, including those that are causative for Joubert Syndrome (JBTS), Meckel-Gruber Syndrome (MKS) and Senior-Loken Syndrome, give highly related clinical phenotypes (9). However, advanced sequencing strategies revealed that mutations in known NPHP-related genes were identified in only 25% of 120 patients, suggesting that a large number of causative genes are yet to be identified (10). Indeed, a recent proteomic analysis defined a network of proteins interacting with NPHP, JBTS and MKS proteins, and patient DNA sequencing identified two new NPHP–JBTS genes (11).

One of the NPHP genes, *NPHP9*, encodes the never-in-mitosis A (NIMA)-related kinase, Nek8. This protein has an N-terminal catalytic domain typical of serine/threonine kinases and a C-terminal domain that bears homology to the seven-bladed β-propeller of the RCC1 GTPase exchange factor. The NIMA-related kinases, or Neks, represent a large family of 11 serine/threonine protein kinases, named Nek1 to Nek11, that are related to the mitotic regulator, NIMA, of the filamentous fungus, *Aspergillus nidulans* (12). Like their fungal counterpart, the human kinases have mainly been studied in relation to their role in cell cycle progression. In particular, Nek2, Nek6, Nek7 and Nek9 clearly function in mitosis, contributing to the separation of centrosomes and establishment of a robust microtubule-based mitotic spindle. Interestingly, though, studies of NIMA-related kinases in other lower eukaryotes, notably *Chlamydomonas* and *Tetrahymena*, revealed potential roles in cilia length control, as well as coordination of ciliogenesis with cell cycle progression (13–15). In this sense, the fact that some Neks play roles in centrosome regulation in mitosis, while others regulate basal body function during ciliogenesis is intriguing and suggests an underlying conserved role in regulation of microtubule organization.

In 2000, the mutation that was causative for two mouse models of polycystic kidney disease, named *kat* (for kidney, anemia, testis) and kat^{2J}, was mapped to the murine Nek1 gene (16,17). This was the first clue that mammalian Neks may have a role in ciliogenesis. Nek1 has since been localized to centrosomes and the primary cilium and has recently been found to be mutated in a human ciliopathy, short-rib polydactyly syndrome type Majewski (18–21). Subsequent to the identification of the mouse Nek1 PKD model, a missense mutation (G448V) in the non-catalytic domain of Nek8 was identified in the *jck* (juvenile cystic kidney) mouse model of autosomal recessive juvenile PKD (22). The kidneys of these mice had significantly lengthened cilia, suggesting that Nek8 might also play a role in ciliary length control (23,24). Otto *et al*. (25) then reported three NPHP families in which mutations in human Nek8 were detected. These included a homozygous H425Y mutation, a heterozygous A497P mutation and a heterozygous L330F mutation that was present in a patient that also had a homozygous mutation in *NPHP5*. The fact that, in two cases, only heterozygous mutations were found in what is a recessive disease suggests that Nek8 may act as a modifier gene in renal and eye pathologies, and be inherited in an oligogenic manner.

Nek8 localizes to the primary cilium, specifically to the proximal region of the cilium that sits just above the transition zone (24,26). This region, which has been named the inversin compartment, is the site at which another NPHP-disease gene, Inv/NPHP2, is localized. In fact, Inv/NPHP2 appears to anchor NPHP3 and Nek8/NPHP9 to this location (26). Other proteins encoded by NPHP-disease genes, including NPHP1, NPHP4 and NPHP8/RPGRIP1L, localize more precisely to the transition zone, below the region where Nek8/NPHP9, Inv/NPHP2 and NPHP3 localize. Moreover, in *Chlamydomonas*, the NPHP6/CEP290 homologue localizes to the wedge-shaped structures that connect the flagellar membrane with the axonemal microtubule doublets in the transition zone; and mutation leads to an abnormal distribution of proteins within the flagella (27). This has led to the hypothesis that the NPHP proteins may exist in one or several complexes around the transition zone that act as gatekeepers to control protein entry and exit from the cilium (28,29).

To date, the kinase activity of Nek8 has not been reported. For this reason, it is difficult to know whether mislocalization of certain Nek8/NPHP9 point mutants is a result of loss of activity. Similarly, it is unclear what role kinase activity has in Nek8 localization, although a point mutant in the mouse Nek8 kinase domain that is predicted to cause loss of activity prevented Nek8 from localizing to cilia (30). Here, we set out to establish an assay that would allow us to measure Nek8 kinase activity in mammalian cells. From this, we propose a model for how activity regulates Nek8 localization based on

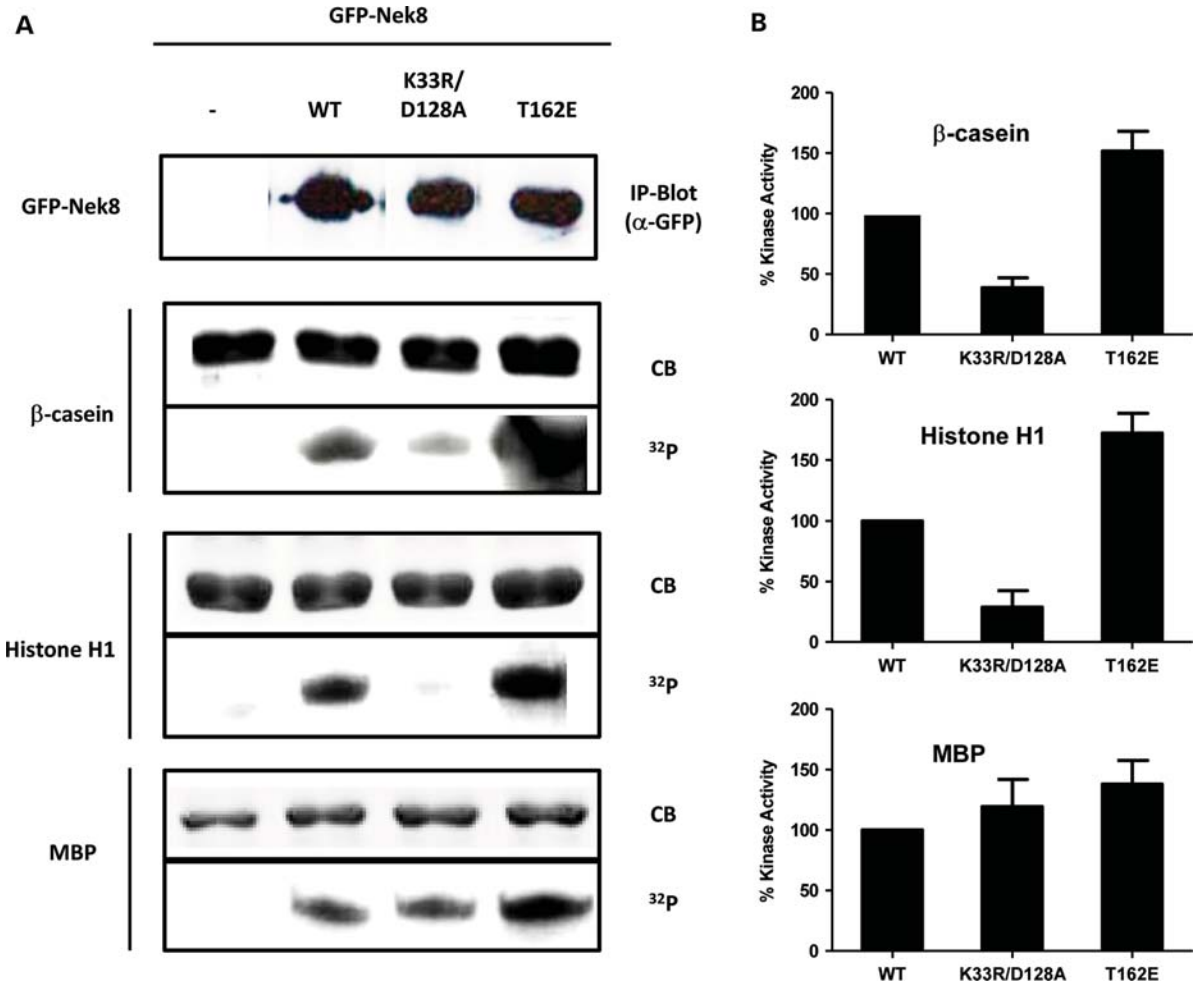

Figure 1. Establishment of Nek8 kinase activity assay. (**A**) HEK 293 cells were either mock transfected (−) or transiently transfected with GFP-tagged Nek8 constructs, as indicated, for 24 h before cells were lysed and immunoprecipitates prepared with anti-GFP antibodies. The amount of kinase precipitated was determined by western blot with anti-GFP antibodies (IP-Blot) and the immunoprecipitates used for kinase assays with β-casein, Histone H1 or MBP as substrates. Samples were analysed by sodium dodecyl sulphate-polyacrylamide gel electrophoresis (SDS–PAGE), Coomassie Blue staining (CB) and autoradiography (^{32}P). (**B**) Kinase activity of Nek8 proteins relative to the wild-type against the different substrates are shown. Data represent means (±SD) of three separate experiments.

the hypothesis that autophosphorylation within the non-catalytic RCC1-like domain is required to expose a ciliary-targeting site present within this domain. Our studies also reveal that Nek8 mutations identified in NPHP patients do not alter activity. Finally, we show that the onset of ciliogenesis is accompanied by activation and proteasomal mediated degradation of Nek8.

RESULTS

Establishment of an assay for Nek8 protein kinase activity

As we wanted to explore the mechanism of Nek8 regulation and how kinase activity might be important for Nek8 function, we first needed to establish conditions under which Nek8 activity could be measured. For this purpose, we began by performing *in vitro* kinase assays using a commercial source of purified GST-tagged Nek8 kinase expressed in wheat germ extract. Using myelin basic protein (MBP), histone H1 or β-casein as model substrates, we found that Nek8 could phosphorylate all these proteins in the presence of 4 μM ATP (Supplementary Material, Fig. S1A and B). The related kinase, Nek9, was shown to require pre-incubation with ATP to activate the kinase before it was capable of phosphorylating exogenous substrates (31). In the case of Nek8, though, we did not find that pre-incubation of the commercial kinase with ATP significantly changed its activity towards these proteins (Supplementary Material, Fig. S1C and D). We then moved on to measure the kinase activity of recombinant GFP-tagged Nek8 expressed in HEK 293 cells. As controls, we generated two different mutants; the first, Nek8-K33R/D128A, had changes in two key catalytic residues that we predicted would lead to loss of activity, and the second, Nek8-T162E, in the activation loop of the catalytic domain, which might be constitutively active. Following transient expression, these proteins were immunoprecipitated with anti-GFP antibodies and incubated under the same assay conditions as the commercial kinase.

The wild-type, but not the catalytically inactive mutant, was capable of phosphorylating β-casein and histone H1, while the T162E mutant showed elevated activity against these substrates (Fig. 1A and B). However, MBP was equally phosphorylated by all three Nek8 constructs, suggesting that this phosphorylation may be attributable to a contaminating kinase. Importantly, while we again found that pre-incubation of the immunoprecipitates with ATP did not alter Nek8 activity, we did find that freezing cell extracts prior to immunoprecipitation led to much reduced activity (data not shown). We therefore conclude that, using these conditions, recombinant Nek8 activity can be assayed following expression in human cells.

NPHP-disease mutants of Nek8 are active

We then used this assay to determine the kinase activity of the three NPHP-disease mutants of Nek8, L330F, H425Y and A497P, previously identified in an analysis of 188 NPHP patients (25). These were generated as GFP-tagged full-length Nek8 constructs for expression in cells (Fig. 2A). In addition, we generated a Nek8-G442V mutation, which was equivalent to the G448V mutation identified in *jck* mice, an A197P mutation, which is an amino acid change reported as a potential driver mutation in pancreatic cancer (32), and a T162A mutation to block phosphorylation at this site within the activation loop. Following expression in HEK 293 cells, these proteins were immunoprecipitated and their activity measured against histone H1 as substrate. All the NPHP-disease mutants, as well as the jck equivalent mutation, G442V, exhibited similar activity to the wild-type protein (Fig. 2B and C). The A197P pancreatic cancer mutant had slightly reduced activity; in contrast, the T162A mutant was completely inactive. We conclude that Nek8 activity is most likely regulated through activation loop phosphorylation and that the NPHP-disease mutants identified to date do not lead to loss of kinase activity.

We next generated GFP-tagged fragments of Nek8 representing the kinase domain alone (GFP-Kin) or the non-catalytic RCC1-like domain (GFP-RCC1). Following expression and immunoprecipitation from HEK 293 cells, we found that the isolated kinase domain showed similar levels of activity to the wild-type protein, while the RCC1 domain had no activity, as expected (Fig. 2D and E). While observing substrate phosphorylation by Nek8, weak autophosphorylation was sometimes apparent. We therefore tested whether the commercial Nek8 kinase was capable of phosphorylating the C-terminal RCC1 domain. Using immunoprecipitates from HEK 293 cells transfected either with GFP alone or GFP-RCC1 as the substrate, we found that Nek8 very efficiently phosphorylated the RCC1 domain (Fig. 2F). We therefore conclude that, under these conditions, the kinase domain alone is sufficient for activity, the kinase domain can phosphorylate the RCC1 domain in trans and the RCC1 domain is not inhibitory of activity in the full-length kinase.

Localization of Nek8 to centrosomes and cilia is dependent on kinase activity and the RCC1 domain

Having established the activity of the different Nek8 constructs, we next examined their localization, specifically in terms of their ability to localize to centrosomes in dividing cells and cilia in serum-starved quiescent cells. For these experiments, the Nek8 proteins were expressed in human hTERT-RPE1 cells, as they form primary cilia upon serum starvation and exit from the cell cycle. As previously found in mouse IMCD-3 cells (30), the wild-type Nek8 protein localized to centrosomes during interphase of dividing cells and to the proximal region of the cilia in ciliated cells, whereas the catalytically inactive mutant failed to localize to either of these sites (Fig. 3A–D). Moreover, in line with our activity measurements, the T162A mutant did not localize to centrosomes or cilia, while the T162E mutant did (Fig. 3A–D). Taken together, these data provide persuasive evidence that Nek8 kinase activity is essential to enable correct localization at centrosomes and cilia.

It has previously been reported that at least some of the NPHP-disease mutants exhibit aberrant localization (25). Having established that all the disease mutants are active and that activity is key to localization, we re-investigated the localization of these mutants. We found that the L330F and A497P mutants localize correctly at centrosomes and cilia, whereas the H425Y and G442V mutants do not (Fig. 3A–D). Interestingly, the A197P mutation discovered in pancreatic cancer also exhibited loss of localization from centrosomes and cilia (Supplementary Material, Fig. S2A and B). This indicates that activity alone is insufficient for correct localization. We therefore examined the localization of the isolated kinase domain and RCC1 domain fragments. In this case, we found that the RCC1 domain localized to centrosomes and cilia, while the kinase domain alone, despite being active, did not (Fig. 4A–D). Taken together, we conclude that the correct localization of full-length Nek8 to centrosomes and cilia requires Nek8 catalytic activity, but that the centrosome/cilia-targeting motif is present within the non-catalytic RCC1 domain. This provides an explanation for why some mutations, but not others, in the RCC1 domain disturb localization. Moreover, as the two mutants that disturb localization, H425Y and G442V, lie close together, we propose that they likely fall within the same targeting motif.

Nek8 proteins also localize to the nucleus

While observing the localization of recombinant Nek8 to the centrosome, we noted that the non-centrosomal pool of protein tended to be equally distributed between the cytoplasm and nucleus. This was also true of the endogenous protein as indicated with a polyclonal antibody that we raised to Nek8, which also showed localization to centrosomes and the proximal region of cilia (Fig. 5A and Supplementary Material, Fig. S3A and B), and for both GFP-Nek8 and Flag-Nek8 (Fig. 5B and data not shown). To test whether this was a regulated event, cells transfected with GFP-Nek8 were treated with leptomycin B, an inhibitor of Crm1-mediated nuclear export. This led to enhanced intensity of the nuclear localization, indicating that Nek8 normally undergoes nuclear-cytoplasmic shuttling (Fig. 5B). We next determined whether the kinase domain or NPHP-disease mutants were altered in their ability to localize to the nucleus. None of the mutations in the kinase domain affected nuclear localization, indicating that activity is not required for nuclear uptake. However,

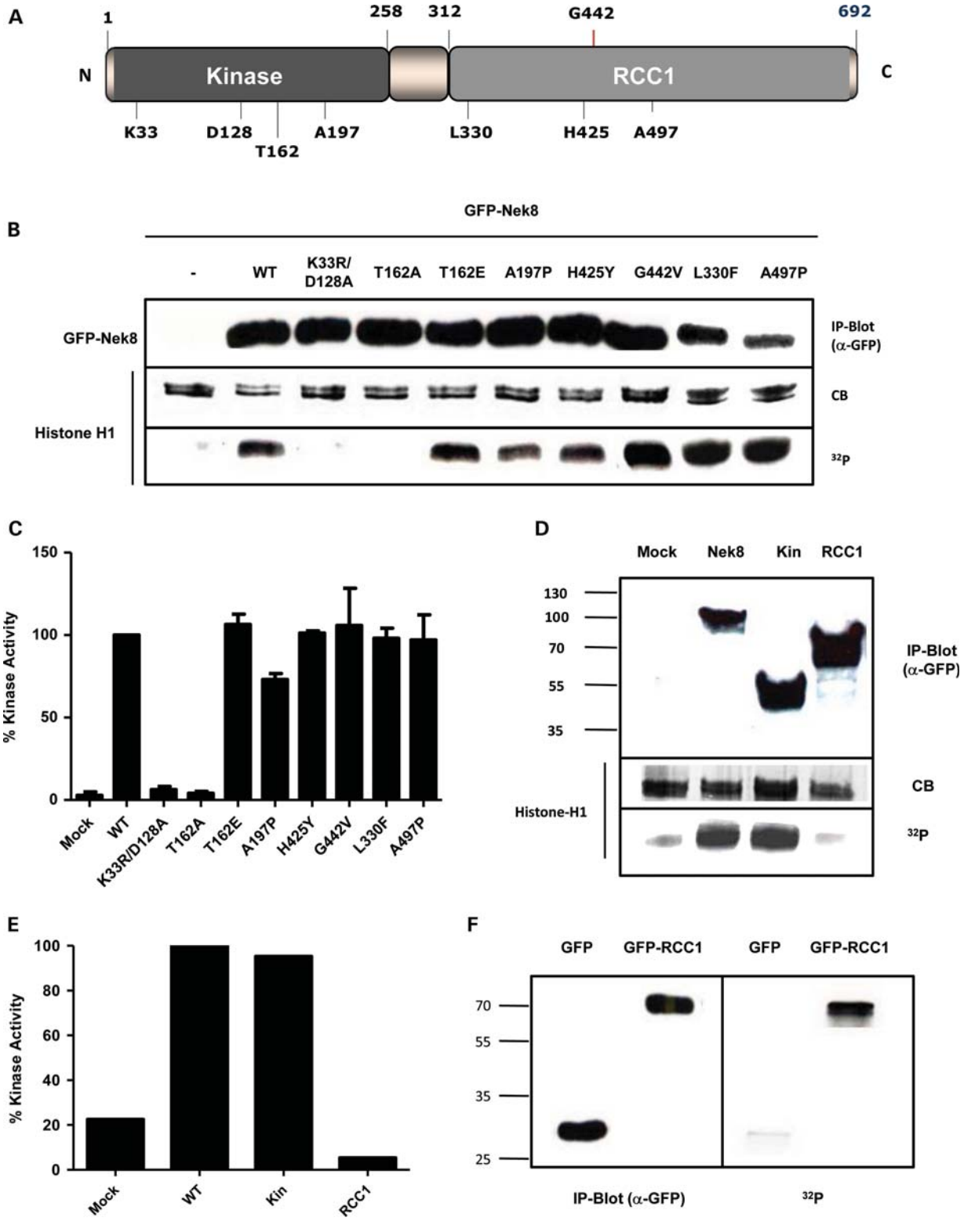

Figure 2. NPHP-disease mutants of Nek8 retain full kinase activity. (**A**) Schematic diagram of Nek8 showing the N-terminal kinase and C-terminal RCC1-like domains. The start and end positions as well as the amino acids mutated in this study are indicated. (**B**). Kinase assays were performed and analysed as described in Figure 1 on immunoprecipitates prepared from HEK 293 cells transfected for 24 h with the constructs indicated and using histone H1 as substrate. (**C**) The kinase activity of the different Nek8 proteins relative to the wild-type is indicated. (**D**) Kinase assays were performed and analysed as described in Figure 1 on immunoprecipitates prepared from HEK 293 cells that were either mock-transfected or transfected for 24 h with wild-type Nek8, the kinase domain fragment (Kin) or the RCC1 domain fragment (RCC1). (**E**) The kinase activity of the different Nek8 proteins relative to the wild-type is indicated. (**F**) HEK 293 cells were transiently transfected with GFP alone or GFP-RCC1 for 24 h before cells were lysed and immunoprecipitates prepared with anti-GFP antibodies. Immunoprecipitates were then subject to western blot with anti-GFP antibodies (IP-Blot) or used in kinase assays with the commercial Nek8 protein. Kinase assays were then subject to SDS–PAGE and autoradiography (^{32}P). Data in (C) and (E) represent means ($\pm$ SD) of three separate experiments. Molecular weights (kDa) are indicated on the left of gels in (D) and (F).

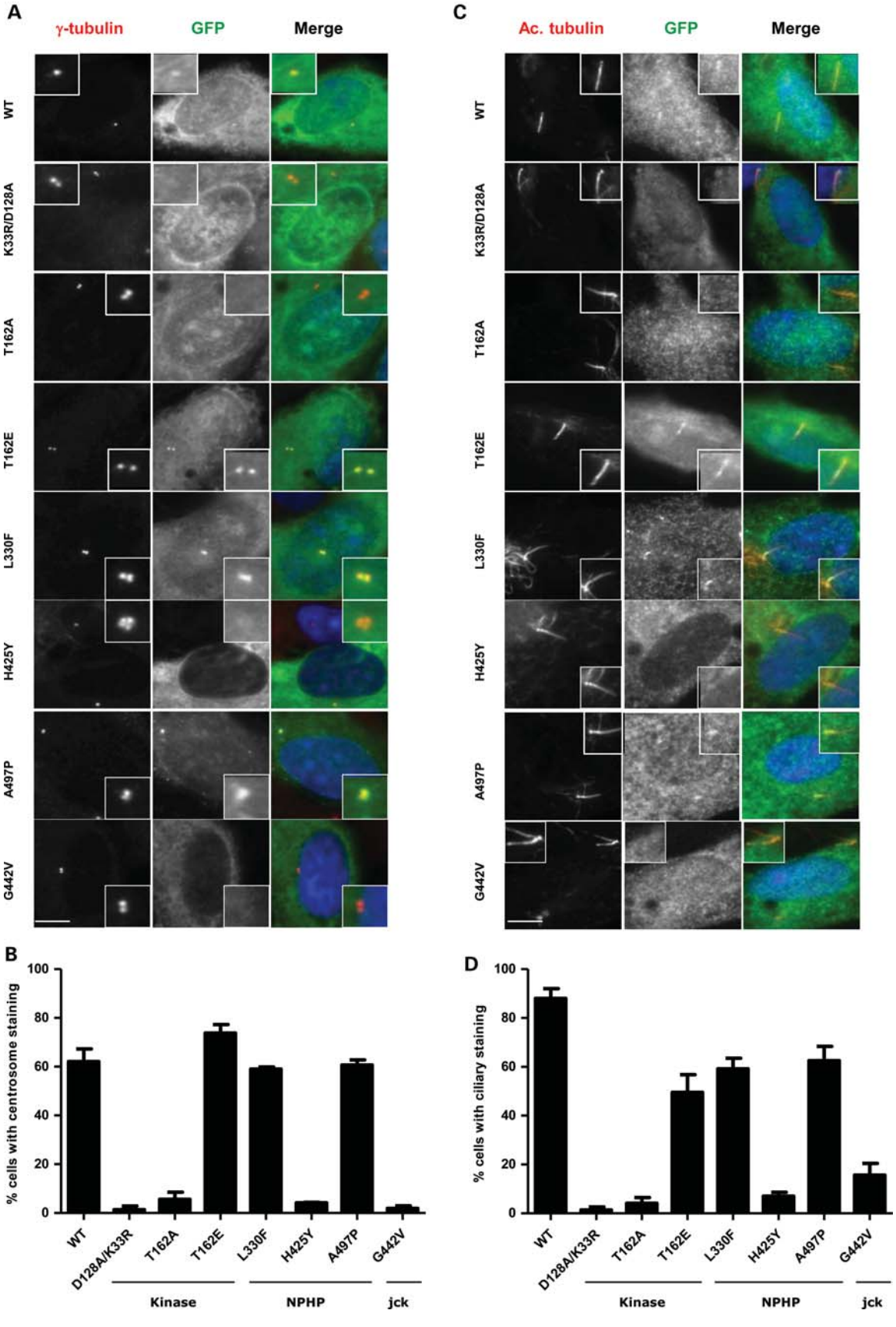
A
γ-tubulin
GFP
Merge
WT
K33R/D128A
T162A
T162E
L330F
H425Y
A497P
G442V
C
Ac. tubulin
GFP
Merge
WT
K33R/D128A
T162A
T162E
L330F
H425Y
A497P
G442V
B
% cells with centrosome staining
100
80
60
40
20
0
WT
D128A/K33R
T162A
T162E
L330F
H425Y
A497P
G442V
Kinase
NPHP
jck
D
% cells with ciliary staining
100
80
60
40
20
0
WT
D128A/K33R
T162A
T162E
L330F
H425Y
A497P
G442V
Kinase
NPHP
jck

while the L330F and A497P mutants localized normally to the nucleus, the H425Y and G442V mutants were both excluded from the nucleus (Fig. 5C and D). The A197P pancreatic mutant also failed to localize to the nucleus (Supplementary Material, Fig. S2C). Upon testing the isolated fragments, we found that the kinase domain alone was excluded consistent with activity not being the key determinant of nuclear uptake, whereas the RCC1 domain did localize to the nucleus (Fig. 5E and F). We interpret these data to mean that one or more nuclear localization sequences (NLS) are present within the non-catalytic RCC1 domain, but that these are disturbed by a number of NPHP point mutations, as well as for some reason, the A197P mutation in the kinase domain.

Nek8 undergoes proteasomal degradation in response to quiescence

During these studies into Nek8 localization, we noted that it was difficult to find transiently transfected cells following serum starvation of hTERT-RPE1 cells. Indeed, calculation of transfection efficiency by immunofluorescence microscopy revealed that, relative to the level seen after 24 h without serum starvation, there was a 5-fold decrease in cells transfected after 24 h serum starvation (Fig. 6A). This loss, which was specific to the GFP-Nek8 protein as it was not seen with GFP alone or GFP-Nek2 (data not shown), was confirmed by western blot analysis (Fig. 6B). To determine whether the sudden loss of Nek8 protein was due to proteasome-mediated degradation, transfected cells were treated with the proteasome inhibitor, MG132, for 4 h following 20 h of serum starvation. This led to a dramatic recovery of both number of transfected cells observed by immunofluorescence microscopy and protein abundance by western blot (Fig. 6A and B). Using Nek8 antibodies, we found that endogenous Nek8 protein also underwent proteasomal degradation upon serum starvation of hTERT-RPE1 cells (Fig. 6C). We wanted to know whether this was a cell cycle response due to entry into quiescence, or a signalling response due to growth factor withdrawal. For this purpose, we transfected GFP-Nek8 into two cell lines, hTERT-RPE1 and NIH3T3, that we confirmed by flow cytometry and BrdU incorporation exited the cell cycle upon serum withdrawal, and two cell lines, HeLa and U2OS, that remained in the cell cycle despite serum withdrawal (Supplementary Material, Fig. S4A–D). Strikingly, we found that the proteasomal-dependent loss of Nek8 only occurred in the cell lines that entered quiescence, and not in those that remained in the cell cycle (Fig. 6D). We then used the different mutant constructs to test whether kinase activity was required for proteasomal degradation and whether the NPHP-disease-associated mutants were also degraded upon serum starvation. All full-length Nek8 constructs were degraded in a proteasome-dependent manner irrespective of whether they had activity or not, or whether they were causative for disease or not (Supplementary Material, Fig. S5A and B). Consistent with this, we found that the kinase domain alone could be degraded in a proteasome-dependent manner and again this was not dependent on activity, as similar results were seen with the kinase domain fragment into which the T162A mutation had been introduced (Fig. 6E and F). Intriguingly, an upshift was seen with the kinase domain fragment alone upon serum starvation that was not present with the T162A mutant, suggesting that serum starvation is also accompanied by phosphorylation at this residue. We therefore conclude that exit from the cell cycle is accompanied by proteasome-mediated degradation of Nek8 that occurs via targeting of the kinase domain but in a kinase-independent manner.

Nek8 kinase is activated upon exit from the cell cycle

Due to the apparent phosphorylation of Nek8 that we had detected upon serum starvation, we then asked whether serum starvation led to a change in activity of the Nek8 kinase. For this purpose, we first attempted to measure GFP-Nek8 activity by immunoprecipitation from transfected hTERT-RPE1 cells, as opposed to HEK 293 cells. Initial attempts to detect Nek8 activity in this manner proved frustrating with similar levels of weak activity being detected with both the wild-type and catalytically inactive Nek8 proteins. However, when cells were serum starved, specific activity from the wild-type, but not catalytically inactive mutant, was detected despite the reduction in protein due to proteasomal degradation (Supplementary Material, Fig. S6A and B). We therefore repeated these experiments adding MG132 to the serum-starved cells and confirmed the dramatic activation of Nek8 in response to exit from the cell cycle (Fig. 7A and B). MG132 did not, on the other hand, stimulate Nek8 activity in the absence of serum starvation (data not shown). Albeit relatively weak, we were also able to detect significant activation of endogenous Nek8 upon serum starvation of hTERT-RPE1 cells (Supplementary Material, Fig. S6C). As we had shown that all the NPHP-disease mutants were active in HEK 293 cells, we tested whether there was any change in activation of these proteins upon serum starvation in hTERT-RPE1 cells. All three of the NPHP-disease-associated mutants, together with the *jck* equivalent mutation and the pancreatic cancer-associated mutation, showed equivalent kinase activation to the wild-type protein (Supplementary Material, Fig. S6D). Finally, as we had found that Nek8 was most likely phosphorylated on T162 upon serum starvation, we asked whether this activation might at least in part be due to phosphorylation at this site. For this purpose, we tested the relative activation of the wild-type and T162

Figure 3. Localization of Nek8 to centrosomes and cilia is dependent on kinase activity. (**A**) Asynchronous hTERT-RPE1 cells were transiently transfected for 24 h with GFP-Nek8 constructs, as indicated. They were fixed in methanol and stained with antibodies against GFP to detect the recombinant Nek8 (green in merge) and γ-tubulin to detect the centrosome (red in merge). (**B**) The histogram shows the % cells with the GFP-Nek8 protein visible at the centrosome. (**C**) hTERT-RPE1 cells were transiently transfected for 4 h with GFP-Nek8 constructs, as indicated, and then serum starved for 48 h to promote ciliogenesis before methanol fixation and staining with antibodies against GFP to detect the recombinant Nek8 (green in merge) and acetylated tubulin to visualize the cilia (red in merge). (**D**) The histogram shows the % cells with the GFP-Nek8 protein visible at the primary cilium. In (A) and (C), DNA was stained with Hoechst 33258 (blue in merge); insets show enlargements of the cilia; scale bars, 10 μm. In (B) and (D), data represent mean (±SD) of three separate experiments where at least 45 cells were counted.

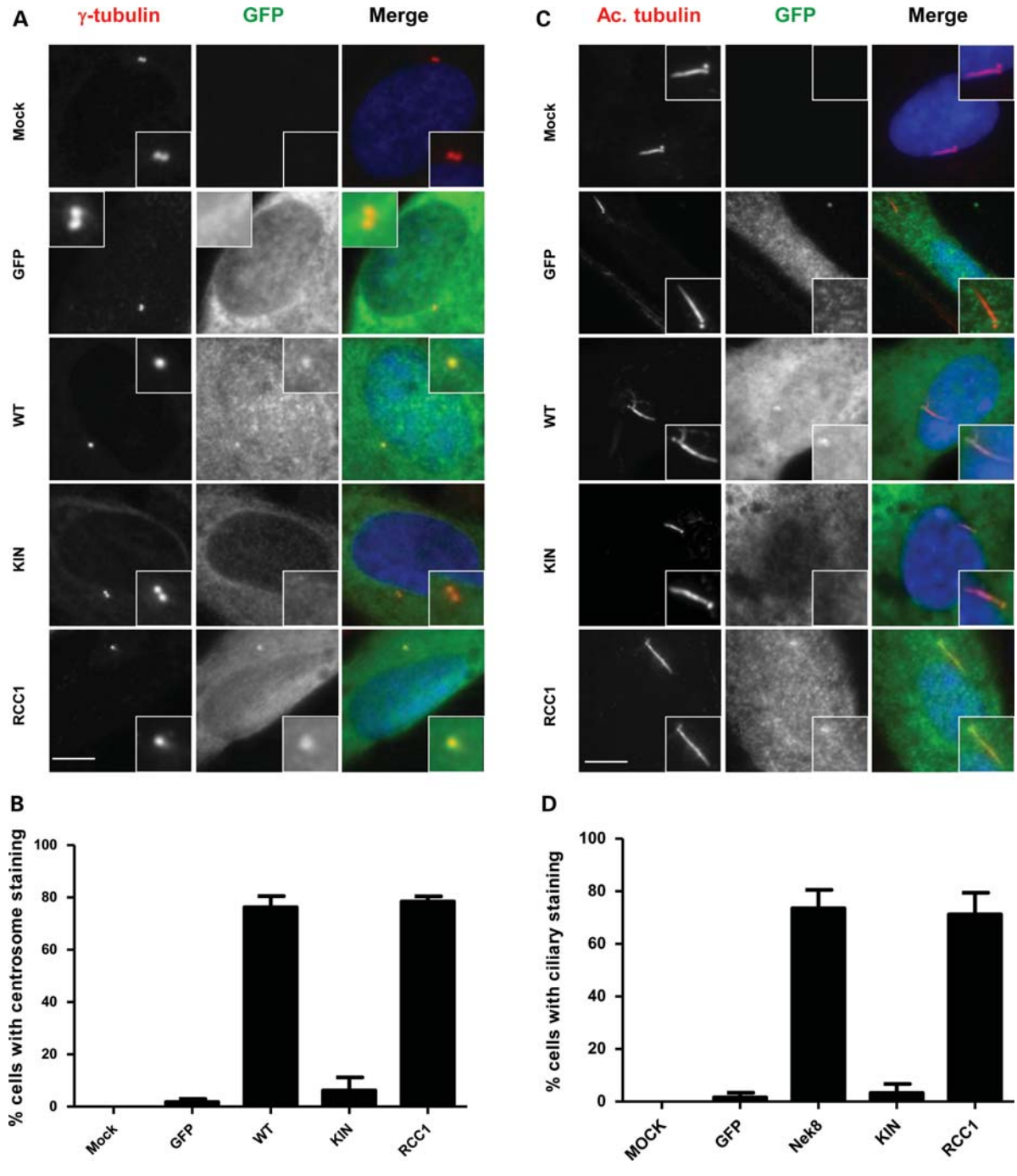

Figure 4. Localization of Nek8 to centrosomes and cilia is regulated by the RCC1 domain. (**A**) hTERT-RPE1 cells were either mock transfected or transiently transfected for 24 h with GFP-Nek8-truncated constructs, as indicated. They were fixed in methanol and stained with antibodies against GFP to detect the recombinant Nek8 (green in merge) and γ-tubulin to detect the centrosome (red in merge). (**B**) The histogram shows the % cells with the GFP-Nek8 protein visible at the centrosome. (**C**) hTERT-RPE1 cells were transiently transfected for 4 h with GFP-Nek8 constructs, as indicated, and then serum starved for 48 h to promote ciliogenesis before methanol fixation and staining with antibodies against GFP to detect the recombinant Nek8 (green in merge) and acetylated tubulin to visualize the cilia (red in merge). (**D**) The histogram shows the % cells with the GFP-Nek8 protein visible at the primary cilium. In (A) and (C), DNA was stained with Hoechst 33258 (blue in merge); insets show enlargements of the cilia; scale bars, 10 μm. In (B) and (D), data represent mean (±SD) of three separate experiments where at least 45 cells were counted.

mutants upon serum starvation. Strikingly, we found that the T162A mutant exhibited very low activity and was not further activated by serum starvation, whereas the T162E mutant showed high activity but was also not further activated (Fig. 7C and D). Moreover, the level of activity of the T162E mutant in cycling cells was similar to that of the wild-type protein after serum starvation. We therefore conclude that exit from the cell cycle is accompanied by activation of Nek8 that largely results from phosphorylation of T162 in the activation loop of the kinase.

DISCUSSION

Here, we describe an assay for Nek8 kinase activity that has allowed us to explore the mechanisms through which this protein implicated in the human juvenile cystic kidney disease, NPHP, is regulated. We found that none of the Nek8 mutations identified in NPHP patients, nor the equivalent mutation to that found in the *jck* mouse model of juvenile cystic kidney disease, alter activity of this enzyme. However, kinase activity is required for correct localization of the protein to the centrosome in dividing cells and the proximal region of the cilia in quiescent cells. On the other hand, localization is mediated via the non-catalytic RCC1 domain, and so we propose that autophosphorylation within this domain may be required to reveal a centrosome-targeting site. We also show that exit from the cell cycle and initiation of ciliogenesis is accompanied by, first, activation and, second, degradation of the Nek8 protein, while activation may require autophosphorylation within the catalytic domain of the kinase. These studies therefore provide important new insights into what regulates both the activity and the localization of this ciliopathy disease protein (Table 1).

We first of all found that mutations not only of key catalytic site residues (K33R and D128A) but also of a site on the activation loop that is often subject to phosphorylation in protein kinases, T162A in the case of Nek8, completely abolished Nek8 kinase activity. Conversely, a T162E phosphomimetic mutant led to equivalent, possibly even elevated, Nek8 activity compared with the wild-type protein. We therefore conclude that Nek8 is almost certainly regulated in a positive manner through phosphorylation at this site. Secondly, we found that an isolated kinase domain was as active as the full-length protein arguing that, unlike the related Nek9 protein (31), either the RCC1-like domain does not act as an auto-inhibitory region, or the auto-inhibition is fully released when the protein is expressed in cycling HEK 293 cells. Thirdly, we found that the full-length kinase was capable of phosphorylating an isolated RCC1-like domain raising the prospect that this kinase undergoes autophosphorylation within this region. When we looked at the localization of these mutant and truncated proteins, we found that localization to the centrosomes and cilia correlated precisely with activity of the full-length proteins (active proteins localizing correctly and inactive proteins failing to localize). Interestingly though, the isolated RCC1-like non-catalytic domain localized correctly but the isolated kinase domain did not. Taken together, we propose a model whereby the RCC1-like domain contains a centrosome/ciliary-targeting sequence, but that kinase activity is also required, with autophosphorylation within the RCC1 domain potentially causing a conformational change that reveals the centrosome-targeting site in the full-length protein (Fig. 8A). The fact that localization of Nek8 to the proximal region of the cilium was dependent on the Inv/NPHP2 protein, which also regulates the localization of NPHP3 to the same compartment (26), means that it will be worthwhile testing whether the centrosome-targeting region is forming a complex with one or both of these proteins.

NPHP is a recessive disease and therefore should result from the loss of function of both alleles of an *NPHP* gene. The H425Y mutant was identified in a homozygous state, and we propose that it is the loss of correct subcellular targeting that leads to the disease. The loss of localization of this mutant from cilia and centrosomes agrees with results obtained by Otto *et al*. (25). However, we also see loss of this mutant from the nucleus and so whether the key defect is loss of localization to centrosomes and cilia, or rather the nucleus, is not clear. Nek8 does not contain an obvious NLS suggesting that nuclear uptake is a result of either a cryptic NLS or interaction with a partner that undergoes nuclear trafficking. In terms of ciliary targeting, while Nek8 does not contain FR motifs or acidic clusters that could bind PACS-1 (33,34), it does contain two VxPx motifs that target PC-2 and other ciliary proteins to this structure (35–38). Although these lie within the RCC1 domain construct used here, they are found at the extreme N-terminus of this region immediately after the kinase domain and it is not clear how they would be affected by the H425Y mutation. Moreover, these motifs are not well conserved (Supplementary Material, Fig. S7). Hence, although worthy of mutational analysis, it remains to be shown whether they are functional or not.

It is intriguing that mislocalization to all three subcellular sites is seen not only with the H425Y mutant but also with the *jck* equivalent G442V mutation that lies within the same RCC1 repeat. One can well imagine that centrosome and ciliary targeting are regulated by interaction with one specific partner protein, but could this also target the protein to the nucleus? This possibility is supported by evidence that the nuclear transport factors Ran and importin-β2 play a role in the ciliary targeting of the microtubule motor protein KIF17 via a motif that can act as either a nuclear or ciliary localization sequence (39). That the H425Y mutation does not just lead to gross misfolding of the protein is supported by the fact that it retains full kinase activity, and is activated and degraded upon serum starvation in a similar manner to the wild-type protein. On the other hand, our data suggest that these latter activities are regulated through the kinase domain and so it remains possible that this mutation does cause a significant disturbance to the predicted β-propeller structure of the RCC1 domain. Structural modelling of the Nek8 RCC1-like domain reveals that H425 lies within a conserved motif that is commonly found in the loop between the third and fourth β-strands of RCC1-like propeller blades (Fig. 8B). The conformation adopted by this motif was resolved in the third β-propeller of the E3 ubiquitin ligase HERC2 in which the motif is found twice. This structure indicates that the conserved histidine side chain forms an intramolecular H-bond with the side chain of a conserved Ser or Thr residue also present within this motif (Fig. 8C). Hence, mutation of this residue to tyrosine is likely to disrupt the local structure. Moreover, H425 and G442 lie within a surface region of the protein that is strictly conserved among vertebrates, as expected for a conserved interface (Fig. 8D, Supplementary Material, Fig. S7 and Movie S1).

The L330F and A497P mutations were only detected in the heterozygous state in NPHP patients. Moreover, the patient carrying the L330F mutation was found to also carry a homozygous mutation in *NPHP5* (25). Our studies revealed no differences in kinase activity, localization, activation or degradation of these two mutants when compared with the wild-type protein. This contradicts somewhat the results of

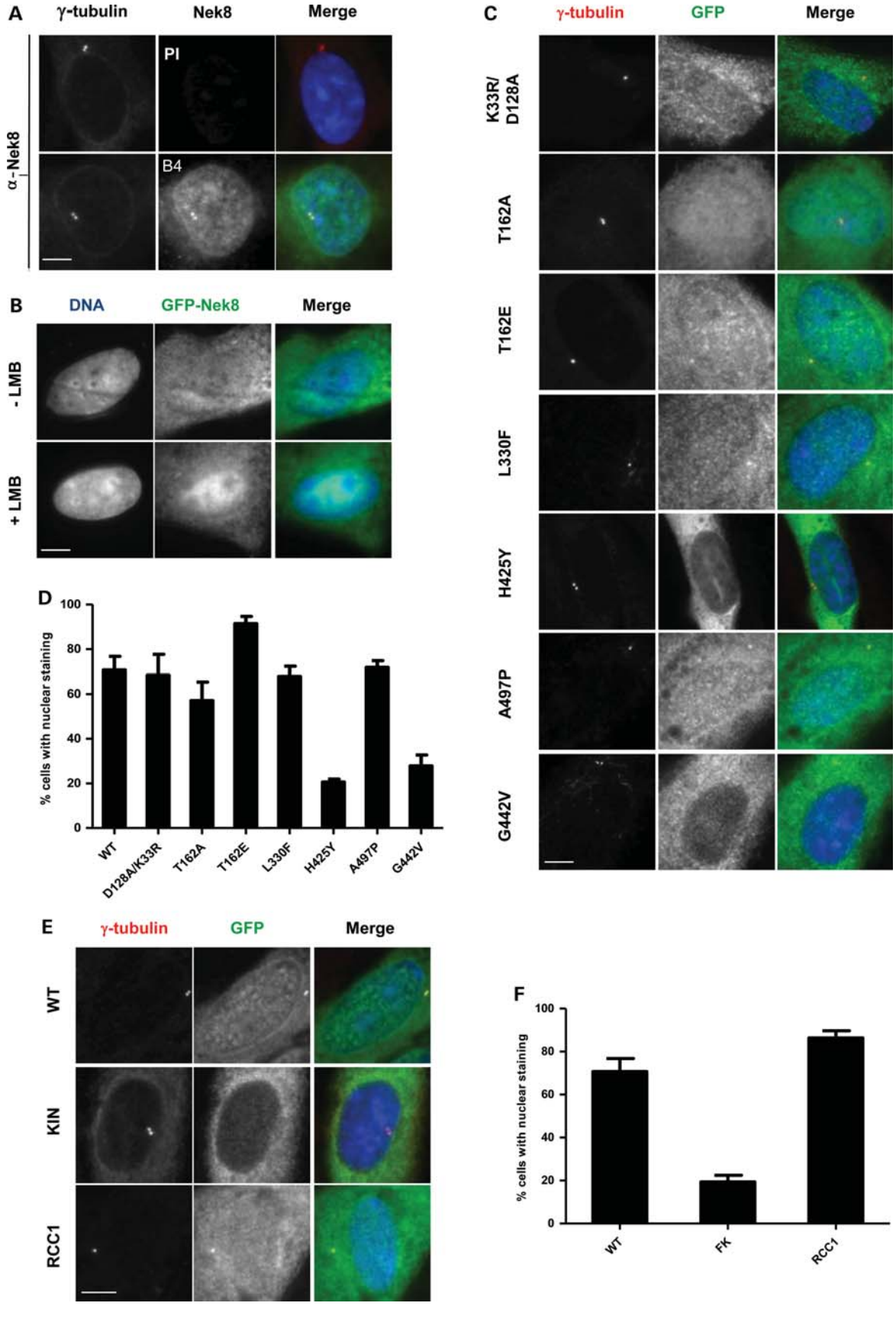
A
γ-tubulin
Nek8
Merge
α-Nek8
PI
B4
B
DNA
GFP-Nek8
Merge
- LMB
+ LMB
C
γ-tubulin
GFP
Merge
K33R/ D128A
T162A
T162E
L330F
H425Y
A497P
G442V
D
% cells with nuclear staining
100
80
60
40
20
0
WT
D128A/K33R
T162A
T162E
L330F
H425Y
A497P
G442V
E
γ-tubulin
GFP
Merge
WT
KIN
RCC1
F
% cells with nuclear staining
100
80
60
40
20
0
WT
FK
RCC1

Otto *et al*. (25) who saw mislocalization of all three NPHP mutants from cilia, but only loss of H425Y from centrosomes. Their experiments though were carried out with mouse Nek8 in IMCD-3 kidney cells, whereas our experiments were performed in human hTERT-RPE1 cells. Whether or not this is the reason for the different results is not clear. However, while it is possible that these mutations act as modifiers in the presence of other bona fide mutations, it remains to be determined whether alone they are capable of causing NPHP.

Our studies identified two key mechanisms of Nek8 regulation that accompanies entry into quiescence and induction of ciliogenesis. First, the Nek8 kinase is activated. This correlates with an upshift that is seen with the kinase domain alone, and which is not seen with a T162A mutant. Furthermore, a T162E mutant is as active in cycling cells as the wild-type protein is after serum starvation. Thus, we propose that the increase in Nek8 kinase activity is a result of activation loop phosphorylation specifically on T162. Whether this is the result of autophosphorylation or an upstream kinase remains to be determined. Secondly, the Nek8 protein undergoes degradation in a proteasome-dependent manner. This was shown with recombinant GFP-Nek8, but not GFP alone, as well as with the endogenous Nek8 protein. Interestingly, degradation appeared to be mediated via the catalytic domain, as the kinase domain alone was also degraded upon serum starvation, but this was not dependent on activity as all full-length kinase domain and disease-associated mutants were degraded. At the present time, the purpose of Nek8 activation and degradation remain entirely unknown. However, we can speculate that Nek8 activity may be required to initiate some aspect of the ciliogenesis programme, whereas its degradation may be required to prevent this initiation process from being maintained indefinitely.

Previous studies have reported that neither siRNA-mediated depletion nor overexpression of Nek8 interferes with ciliogenesis (18,25,30). Understanding why mutation of Nek8 should lead to cystic kidney disease therefore remains an enigma. One possibility is that mislocalization disturbs the gatekeeper function of protein complexes that include some of the NPHP proteins and which localize around the transition zone (28,29). This could lead to an imbalance in the localization of ciliary proteins that control key developmental signalling pathways, such as those mediated by the Hedgehog and Wnt ligands (2,40,41). Similarly, it could disturb signalling via the polycystins, PC-1 and PC-2, that are mutated in ADPKD. Indeed, Nek8 is reported to interact with the PC-2 protein, while the expression and localization of PC-1 and PC-2 are disturbed in renal cells from the *jck* mouse (23,24). In addition, mice that carry heterozygous mutations in both the *Pkd1* gene, which encodes PC-1, and the *Nek8* gene also develop a more aggressive form of cystic kidney disease than are seen in *Pkd1* heterozygotes alone (42). Interestingly, Nek1 is also implicated in regulating PC-2 expression, in this case through phosphorylation of an E3 ubiquitin ligase adaptor that normally targets PC-2 for degradation (43).

Finally, our data with the A197P mutant raise some interesting questions. This mutation lies within the catalytic domain and was identified as a potential driver mutation in pancreatic cancer (32), while overexpression of Nek8 has been reported in breast tumours (44). While we found no dramatic alteration in the kinase activity of this mutant, its ability to localize to the centrosome, cilium and nucleus was completely abolished. This could potentially abrogate a transcriptional programme that dictates whether cells enter quiescence or continue through the cell cycle. Indeed, defects in ciliary signalling to the nucleus have now been implicated in the development of tumours (45,46). Alternatively, Nek8 could play a role at centrosomes during mitotic cell division and it is worth bearing in mind that the development of kidney cysts reflects a loss of control over cell cycle progression and, possibly, mitotic spindle orientation (47–50). Recently, it was found that cells from ARPKD patients that have mutations in the fibrocystin/polyductin protein exhibit centrosome amplification and mitotic spindle defects again linking cystic kidney disease formation with mitotic defects (51). Moreover, whereas one study did not detect Nek8 on centrosomes in dividing cells (18), we and others clearly observed Nek8 on centrosomes throughout the cell cycle and overexpression of Nek8 has been reported to drive multinucleation, indicative of cell division failure (22,30). It is possible then that, like certain other Neks including Nek1 (52), Nek8 has functions in the DNA damage response providing another reason for its nuclear localization. Further studies are clearly required to address how Nek8 might coordinate ciliogenesis with the mitotic cell division cycle.

MATERIALS AND METHODS

Plasmid constructions

Full-length Nek8 (residues 1–692), the kinase domain alone (residues 4–258) and the RCC1 domain (residues 259–692) were amplified by polymerase chain reaction using a full-length human Nek8 cDNA obtained from the German cDNA Consortium (RZPD) (clone DKFZp434NO419) as the template. Amplified fragments were subcloned into the mammalian expression vectors, pEGFP-T7 (53) and pFLAG-CMV-2 (Sigma), and the bacterial expression vector, pETM-11 (gift from EMBL, Heidelberg), providing N-terminal GFP, Flag or His tags, respectively. Site-directed mutagenesis was

Figure 5. Nek8 proteins shuttle to the nucleus in an RCC1-dependent manner. (**A**) Asynchronous hTERT-RPE1 cells were fixed in methanol and stained with antibodies against Nek8 (pre-immune sera, PI, top row; or immune sera bleed 4, B4, bottom row; green in merge) and γ-tubulin to detect the centrosome (red in merge). (**B**) hTERT-RPE1 cells were transiently transfected with GFP-Nek8 for 24 h and then treated without (−LMB) or with (+LMB) leptomycin B for 6 h before being fixed in methanol and stained with GFP antibodies to detect the recombinant Nek8 (green in merge) and Hoechst 33258 to stain the DNA. (**C**). hTERT-RPE1 cells were transiently transfected for 24 h with the Nek8 constructs, as indicated before fixation in methanol and staining with antibodies against GFP to detect the recombinant Nek8 (green in merge) and γ-tubulin to detect the centrosome (red in merge). (**D**) The histogram shows the % cells with GFP-Nek8 either predominantly within the nucleus or with equal staining between cytoplasm and nucleus. (**E**) hTERT-RPE1 cells were transiently transfected for 24 h with the Nek8 constructs as indicated and processed as in (C). (**F**) The histogram indicates nuclear localization of constructs analysed in (E). In (A–C) and (E), DNA was stained with Hoechst 33258 (blue in merge); scale bars, 10 μm. Data in (D) and (F) represent mean (± SE) of three separate experiments where at least 45 cells were counted.

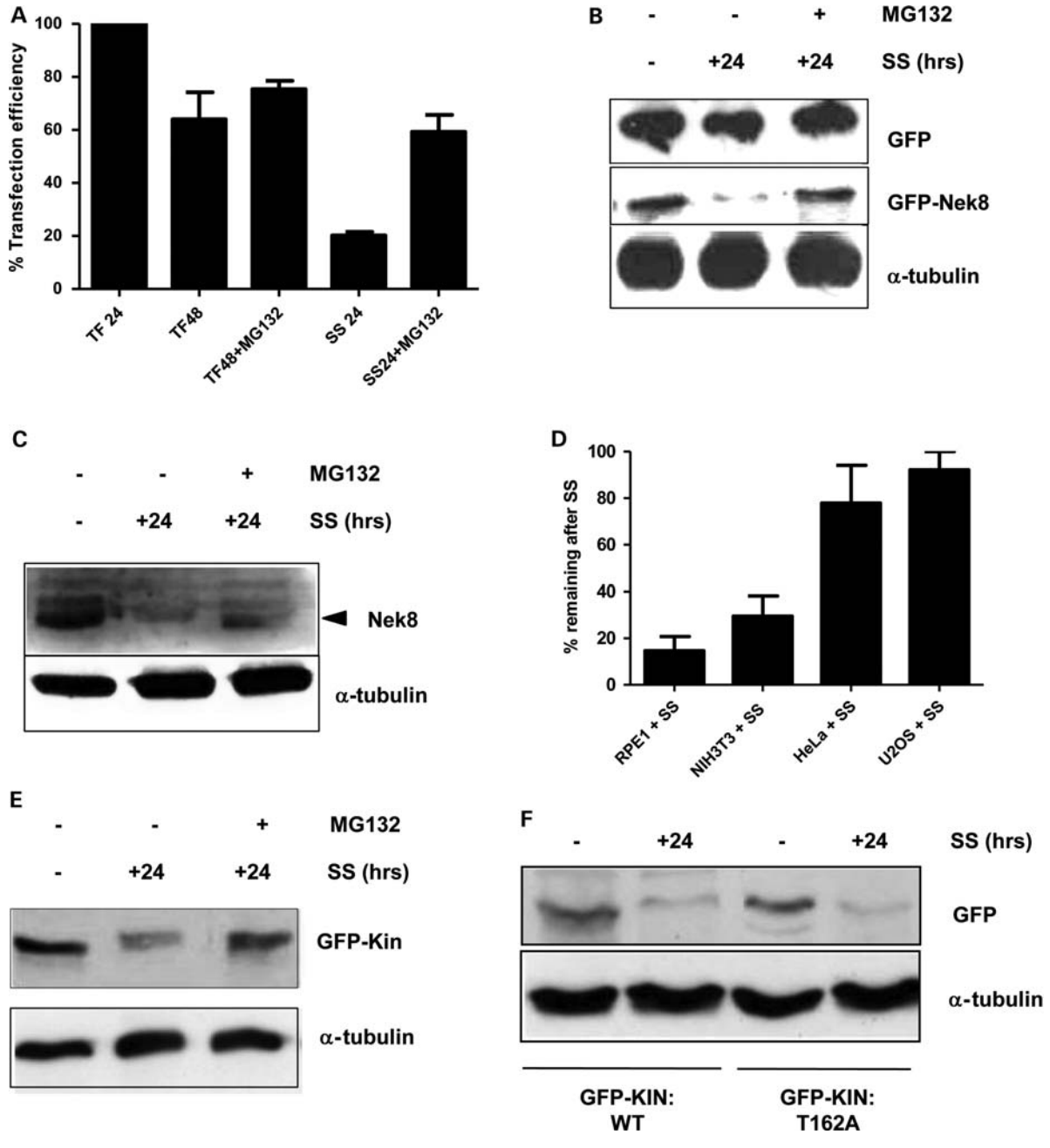

Figure 6. Serum starvation induces proteasomal degradation of Nek8. (**A**) The transfection efficiency (% cells positive for GFP-Nek8 as determined by immunofluorescence microscopy with GFP antibodies) in hTERT-RPE1 cells was determined at the times indicated after transfection (TF, hours), with or without serum starvation (SS) and with or without MG132 treatment, as indicated. (**B**) hTERT-RPE1 cells were transfected with GFP alone or GFP-Nek8 for 48 h and SS and treated with MG132, as indicated. Samples were analysed by SDS–PAGE and western blotting with antibodies against GFP and α-tubulin. (**C**) To observe degradation of endogenous Nek8, hTERT-RPE1 cells were incubated as indicated before analysis by SDS–PAGE and western blotting with antibodies against Nek8 and α-tubulin. (**D**) GFP-Nek8 was transfected into hTERT-RPE1, NIH 3T3, HeLa and U2OS cells. They were then incubated for 48 h with serum or in serum-free media. Extracts were prepared and analysed for the amount of protein remaining after SS, when compared with in the presence of serum, by SDS–PAGE and western blotting with anti-GFP antibodies. (**E**) hTERT-RPE1 cells were transfected for 48 h with the GFP-tagged Nek8 kinase domain alone (GFP-Kin) and SS and treated with MG132, as indicated. Samples were analysed by SDS–PAGE and western blotting with antibodies against GFP and α-tubulin. (**F**) hTERT-RPE1 cells were transfected for 48 h with GFP-tagged wild-type or T162A kinase domain construct and treated as indicated before analysis by SDS–PAGE and western blotting with antibodies against GFP and α-tubulin. Data in (A) and (C) represent means ($\pm$SD) of three separate experiments.

performed using the Genetailor^{TM} Site-Directed Mutagenesis System (Invitrogen) according to the manufacturer's instructions. All constructs were verified by DNA sequencing within the Protein and Nucleic Acid Laboratory (Leicester).

Antibody generation

For production of antibodies against Nek8, rabbits were immunized with a His-tagged C-terminal fragment of Nek8

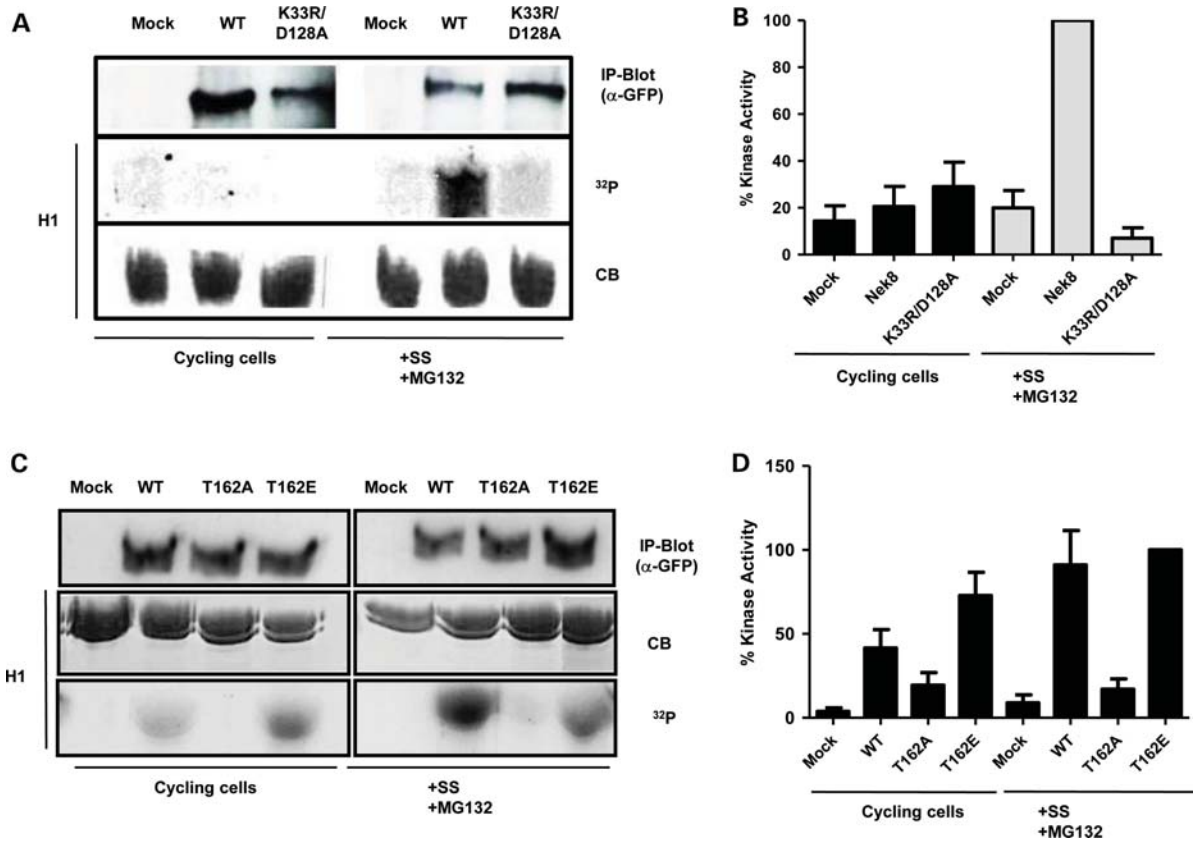

Figure 7. Cell cycle exit induces activation of Nek8. (**A**) hTERT-RPE1 cells were either mock transfected or transiently transfected with wild-type GFP-Nek8 (WT) or GFP-Nek8-K33R/D128A for 48 h and either left in normal media (left three lanes) or serum-starved (SS) for the final 24 h with MG132 addition 4 h prior to harvesting (right three lanes). Cells were then lysed and subjected to immunoprecipitation with anti-GFP antibodies. The amount of kinase precipitated was determined by western blot with anti-GFP antibodies (IP-Blot) and the immunoprecipitates used for kinase assays with histone H1 as substrate. Samples were analysed by SDS–PAGE, Coomassie Blue staining (CB) and autoradiography (^{32}P). (**B**) The kinase activity of Nek8 under different conditions against histone H1 is shown relative to the activity for the wild-type kinase after SS. (**C**) hTERT-RPE1 cells were transfected with the GFP-tagged Nek8 constructs indicated and processed as in (A). (**D**) The kinase activity of samples shown in (C) was determined as in (B). Data in (B) and (D) represent means ($\pm$SD) of three separate experiments.

Table 1. Activity and subcellular localization of kinase domain and disease-associated mutants of Nek8

	Nek8 constructs	Kinase activity	Centrosome	Cilium	Nucleus
Wild-type Nek8	WT	Yes	+	+	+
Isolated fragments	Kinase domain	Yes	−	−	−
	RCC1 domain	No	+	+	+
NPHP9 mutations	L330F	Yes	+	+	+
	H425Y	Yes	−	−	−
	A497P	Yes	+	+	+
jck mutation	G442V	Yes	−	−	−
Catalytic mutants	K33R/D128A	No	−	−	+
	T162A	No	−	−	+
	T162E	Yes	+	+	+
Pancreatic cancer	A197P	Yes	−	−	−

The table summarizes the data obtained in this study on the kinase activity and subcellular localization of different Nek8 constructs based on expression of GFP-tagged constructs in human hTERT-RPE1 cells. Kinase activity and localization to the centrosome and nucleus were determined in asynchronous dividing cells, while localization to the primary cilium was determined in serum-starved ciliated cells. Note that of the three NPHP9-associated mutations, only one was identified in a homozygous state, H425Y, which showed mislocalization from centrosomes, cilia and nuclei. The L330F and A497P mutations were identified as heterozygous mutations and, as NHPH is a recessive disease and we saw no mislocalization of these mutants, it remains unclear what role they have in the disease.

spanning amino acids 270–550. This fragment was expressed in *E. coli* strain Rosetta 2 (DE3) (Novagen) and purified under denaturing conditions according to the standard protocols. Immunizations and affinity purification of antibodies were performed by Cambridge Research Biochemicals.

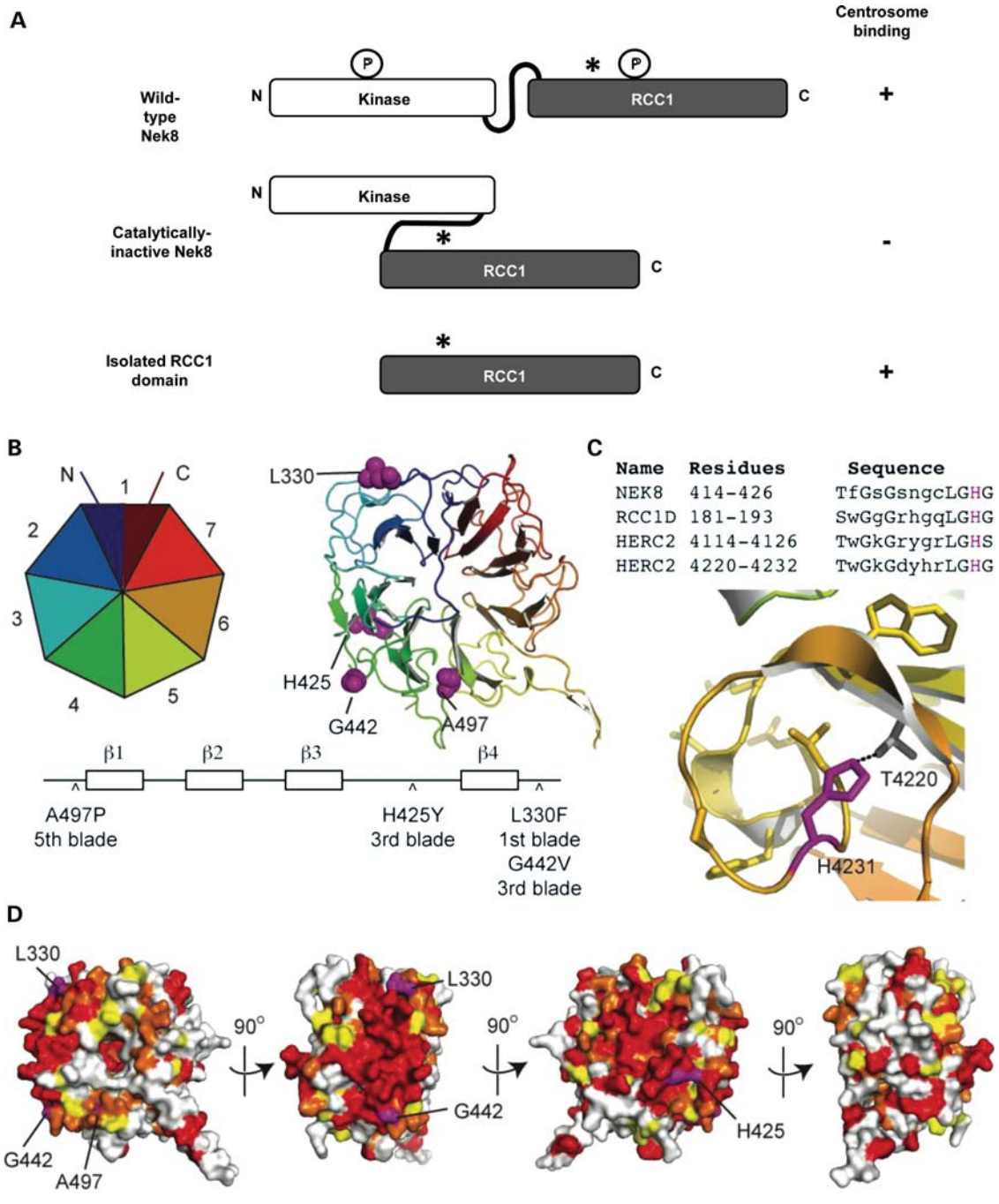

Figure 8. Models of Nek8 structure and regulation. (**A**) The schematic diagram shows how both kinase activity and the non-catalytic RCC1 domain may be required for localization of Nek8 to centrosomes, cilia and possibly, nuclei. In this model, the wild-type protein undergoes autophosphorylation within the RCC1 domain. It also undergoes phosphorylation within the activation loop of the catalytic domain, although whether this is an autophosphorylation event is unclear. We propose that these phosphorylation events lead to an opening up of the conformation that reveals a centrosome-targeting sequence present within the RCC1 domain (*). However, a catalytically inactive mutant cannot autophosphorylate and hence remains in the closed conformation whereby the centrosome-targeting sequence is masked. In an isolated RCC1 domain, the centrosome-targeting site would be unmasked and therefore not require phosphorylation. (**B**) A structural model of the human Nek8 RCC1-like domain (residues 300–692) generated using Phyre and represented in Pymol is predicted to form a 7-bladed β-propeller, shown schematically (above left) and in cartoon representation (above right). The first blade is formed from residues at the N- and C-terminal ends of the domain, the other blades are formed sequentially, and each blade is composed of four beta-strands (below). Residues mutated in human NPHP patients and in the *jck* mouse are shown as magenta spheres on the modelled structure (above right) and their positions within the blade are indicated (below). (**C**) Residue H425 of Nek8 lies within a conserved motif that is commonly found in the loop between the third and fourth β-strands of RCC1-like propeller blades (above). The conformation adopted by this motif was resolved in the third β-propeller of the E3 ubiquitin ligase HERC2 (PDB code 3KCI), in which the motif is found twice. The region around residues 4220–4232 in HERC2 is representative (below), and reveals that the conserved histidine side chain (magenta) forms a H-bond (dashed line) with the side chain of a conserved Ser or Thr residue (grey). (**D**) Four surface views of the human Nek8 RCC1 domain model related by 90° rotations around a vertical axis. With the exception of L330, H425, G442 and A497, which are coloured magenta, the surface is coloured by sequence conservation (as defined in Supplementary Material, Fig. S7): identical residues, red; conserved residues, orange; semi-conserved residues, yellow; non-conserved residues, white. Conserved surface patches that include H425 and G442, which are absolutely conserved, are clearly visible in the two central images, and there are no other extensive areas of surface conservation.

Cell culture and transfections

Cells were grown in the following media: hTERT-RPE1 and NIH 3T3 cells in Dulbecco's modified Eagle's medium (DMEM)/Ham's F12 (1:1) supplemented with 0.348% sodium bicarbonate solution. HEK 293, HeLa and U2OS cells were also gown in the DMEM medium. All cells were supplemented with 10% fetal calf serum, 100 IU/ml penicillin and 100 μg/ml streptomycin. Cells were grown at 37°C in a 5% CO_2 atmosphere. Serum starvation was performed for the times indicated by washing the cells 3× with 1× phosphate-buffered saline (PBS) and replacing with the serum-free medium. Transient transfections were performed with Lipofectamine 2000 (Invitrogen), Fugene HD (Roche) or according to the manufacturer's instructions and analysed after 24 or 48 h. MG132 (Sigma) and LMB (Calbiochem) were added where indicated to a final concentration of 10 μM and 40 nM, respectively.

Immunofluorescence microscopy

Immunofluorescence microscopy was carried out following fixation in cold methanol as previously described (54). Primary antibodies were against Nek8 (1:250 dilution of final bleed), acetylated tubulin (0.5 μg/ml; Sigma), γ-tubulin (0.15 μg/ml, Sigma), GFP (0.5 μg/ml; Abcam) and Flag (1:1000; Cell Signalling). Secondary antibodies were Alexa Fluor 488- and 594-conjugated goat anti-mouse and goat anti-rabbit IgGs (1 μg/ml, Invitrogen). Images were captured using a TE300 inverted microscope (Nikon) or Leica TCS SP5 confocal microscope equipped with a Leica DMI 6000B inverted microscope using a 63× oil objective (numerical aperture, 1.4). BrdU labelling was performed with the BrdU labelling and detection kit II from Roche according to the manufacturer's instructions.

Preparation of cell extracts, SDS–PAGE and western blotting

For kinase assays, cells were lysed in NEB buffer (50 mM HEPES-KOH, pH 7.4, 5 mM $MnCl_2$, 10 mM $MgCl_2$, 5 mM ethylene glycol tetraacetic acid, 2 mM ethylene diamine tetraacetic acid, 100 mM NaCl, 5 mM KCl, 0.1% (v/v) NP-40, 30 μg/ml RNase A, 30 μg/ml DNase I, 10 μg/ml leupeptin, 10 μg/ml bestatin, 10 μg/ml pepstatin, 1 mM PMSF, 20 mM β-glycerophosphate, 20 mM NaF). For degradation experiment, cells were washed once in PBS and lysed in lysis buffer (50 mM Tris·HCl, pH 8.0, 0.5% Nonidet P-40, 150 mM NaCl, 1 mM PMSF, 1× Protease Inhibitor Cocktail) for 30 min on ice. Lysates were centrifuged for 10 min, 13 000 rpm, at 4°C, and protein concentrations of the cleared supernatant determined by the Bradford assay. Sodium dodecyl sulphate-polyacrylamide gel electrophoresis (SDS–PAGE), Coomassie Blue staining and western blotting were performed as previously described (55). For western blots of cell lysates, 20 μg of total protein was loaded per lane. Primary antibodies were against Nek8 (1:250), α-tubulin (0.3 μg/ml; Sigma) and GFP (0.5 mg/ml; Abcam). Secondary antibodies were alkaline-phosphatase-conjugated anti-rabbit or anti-mouse IgGs (1:7500; Promega) or horseradish peroxidase-labelled IgGs (Amersham).

Immunoprecipitations

Four milligrams of transfected cell extracts were pre-cleared for 30 min at 4°C with protein G agarose beads (Sigma) that had been pre-washed in NEB buffer. Beads were then removed and supernatants incubated with GFP antibody (1 mg/ml; Abcam) for 1 h on ice. The complexes were then captured with protein G agarose beads (again pre-washed in NEB buffer) O/N at 4°C. Beads were then prepared for further analysis by washing thrice in NEB buffer.

In vitro kinase assays

Kinase assays were carried out using either 25–30 μl of washed immune complex beads, prepared as described above, or 0.1 μg of purified Nek8 kinase (Novus Biologicals; Littleton, CO, USA). Briefly, proteins were incubated with 5 μg of the appropriate substrate and 1 μCi of [γ-^{32}P]-ATP in 40 μl kinase buffer (50 mM Hepes-KOH, pH 7.4, 5 mM $MnCl_2$, 5 mM β-glycerophosphate, 5 mM NaF, 4 μM ATP, 1 mM DTT) for 30 min at 30°C. To test the requirement for Mg^{2+}, the $MnCl_2$ was substituted for $MgCl_2$. To test the requirement for auto-activation, kinases were pre-incubated in kinase buffer for 1 h at 30°C prior to addition of substrate and radiolabeled ATP. Reactions were stopped by addition of 50 μl 3× Laemmli buffer and analysed by SDS–PAGE and autoradiography. Substrate phosphorylation was quantified by scintillation counting of protein bands excised from dried gels. Excised bands were immersed in 3 ml Optiphase HiSafe 2 liquid scintillant (Wallace-Perkin Elmer) and amount of ^{32}P incorporation determined by quantification in a LS6500 scintillation analyzer (Beckman Coulter).

Flow cytometry

To determine cell cycle distributions, cell populations for analysis were harvested as appropriate, pelleted by centrifugation and washed in 1× PBS before being resuspended in 1 ml 70% ice-cold ethanol to fix cells. Cells were maintained in ethanol at 4°C for a minimum of 30 min before being stained with propidium iodide. Briefly, cells were washed twice in 1× PBS to remove all traces of ethanol, and resuspended in 1× PBS supplemented with 200 μg/ml RNase A and 20 μg/ml propidium iodide. Cells were stained in the dark at 4°C for a minimum of 4 h. Cells were then analysed via flow cytometry, using a FACScan II instrument and CellQuest Pro software (BD Biosciences).

SUPPLEMENTARY MATERIAL

Supplementary Material is available at *HMG* online.

ACKNOWLEDGEMENTS

We are very grateful to Adrian Woolf (Manchester) for critical comments on the manuscript and all members of our laboratory for useful discussion.

Conflict of Interest statement. None declared.

FUNDING

This work was supported by a grant to A.M.F. from The Wellcome Trust (grant number 082828); and a PhD studentship to D.Z. from the Medical Research Council. R.B. is a Royal Society University Research Fellow. Funding to pay the Open Access publication charges for this article was provided by The Wellcome Trust.

REFERENCES

1. Marshall, W.F. and Nonaka, S. (2006) Cilia: tuning in to the cell's antenna. *Curr. Biol.*, **16**, R604–R614.
2. Berbari, N.F., O'Connor, A.K., Haycraft, C.J. and Yoder, B.K. (2009) The primary cilium as a complex signaling center. *Curr. Biol.*, **19**, R526–R535.
3. Badano, J.L., Mitsuma, N., Beales, P.L. and Katsanis, N. (2006) The ciliopathies: an emerging class of human genetic disorders. *Annu. Rev. Genomics Hum. Genet.*, **7**, 125–148.
4. Marshall, W.F. (2008) The cell biological basis of ciliary disease. *J. Cell Biol.*, **180**, 17–21.
5. Baker, K. and Beales, P.L. (2009) Making sense of cilia in disease: the human ciliopathies. *Am. J. Med. Genet. C Semin. Med. Genet.*, **151C**, 281–295.
6. Nigg, E.A. and Raff, J.W. (2009) Centrioles, centrosomes, and cilia in health and disease. *Cell*, **139**, 663–678.
7. Chapin, H.C. and Caplan, M.J. (2010) The cell biology of polycystic kidney disease. *J. Cell Biol.*, **191**, 701–710.
8. Hildebrandt, F., Attanasio, M. and Otto, E. (2009) Nephronophthisis: disease mechanisms of a ciliopathy. *J. Am. Soc. Nephrol.*, **20**, 23–35.
9. Hurd, T.W. and Hildebrandt, F. (2011) Mechanisms of nephronophthisis and related ciliopathies. *Nephron Exp. Nephrol.*, **118**, e9–e14.
10. Otto, E.A., Ramaswami, G., Janssen, S., Chaki, M., Allen, S.J., Zhou, W., Airik, R., Hurd, T.W., Ghosh, A.K., Wolf, M.T. *et al.* (2011) Mutation analysis of 18 nephronophthisis associated ciliopathy disease genes using a DNA pooling and next generation sequencing strategy. *J. Med. Genet.*, **48**, 105–116.
11. Sang, L., Miller, J.J., Corbit, K.C., Giles, R.H., Brauer, M.J., Otto, E.A., Baye, L.M., Wen, X., Scales, S.J., Kwong, M. *et al.* (2011) Mapping the NPHP-JBTS-MKS protein network reveals ciliopathy disease genes and pathways. *Cell*, **145**, 513–528.
12. Quarmby, L.M. and Mahjoub, M.R. (2005) Caught Nek-ing: cilia and centrioles. *J. Cell Sci.*, **118**, 5161–5169.
13. Bradley, B.A. and Quarmby, L.M. (2005) A NIMA-related kinase, Cnk2p, regulates both flagellar length and cell size in Chlamydomonas. *J. Cell Sci.*, **118**, 3317–3326.
14. Mahjoub, M.R., Montpetit, B., Zhao, L., Finst, R.J., Goh, B., Kim, A.C. and Quarmby, L.M. (2002) The FA2 gene of Chlamydomonas encodes a NIMA family kinase with roles in cell cycle progression and microtubule severing during deflagellation. *J. Cell Sci.*, **115**, 1759–1768.
15. Wloga, D., Camba, A., Rogowski, K., Manning, G., Jerka-Dziadosz, M. and Gaertig, J. (2006) Members of the NIMA-related kinase family promote disassembly of cilia by multiple mechanisms. *Mol. Biol. Cell*, **17**, 2799–2810.
16. Upadhya, P., Birkenmeier, E.H., Birkenmeier, C.S. and Barker, J.E. (2000) Mutations in a NIMA-related kinase gene, Nek1, cause pleiotropic effects including a progressive polycystic kidney disease in mice. *Proc. Natl Acad. Sci. USA*, **97**, 217–221.
17. Vogler, C., Homan, S., Pung, A., Thorpe, C., Barker, J., Birkenmeier, E.H. and Upadhya, P. (1999) Clinical and pathologic findings in two new allelic murine models of polycystic kidney disease. *J. Am. Soc. Nephrol.*, **10**, 2534–2539.
18. Mahjoub, M.R., Trapp, M.L. and Quarmby, L.M. (2005) NIMA-related kinases defective in murine models of polycystic kidney diseases localize to primary cilia and centrosomes. *J. Am. Soc. Nephrol.*, **16**, 3485–3489.
19. Shalom, O., Shalva, N., Altschuler, Y. and Motro, B. (2008) The mammalian Nek1 kinase is involved in primary cilium formation. *FEBS Lett.*, **582**, 1465–1470.
20. White, M.C. and Quarmby, L.M. (2008) The NIMA-family kinase, Nek1 affects the stability of centrosomes and ciliogenesis. *BMC Cell Biol.*, **9**, 29.
21. Thiel, C., Kessler, K., Giessl, A., Dimmler, A., Shalev, S.A., von der Haar, S., Zenker, M., Zahnleiter, D., Stoss, H., Beinder, E. *et al.* (2011) NEK1 mutations cause short-rib polydactyly syndrome type majewski. *Am. J. Hum. Genet.*, **88**, 106–114.
22. Liu, S., Lu, W., Obara, T., Kuida, S., Lehoczky, J., Dewar, K., Drummond, I.A. and Beier, D.R. (2002) A defect in a novel Nek-family kinase causes cystic kidney disease in the mouse and in zebrafish. *Development*, **129**, 5839–5846.
23. Smith, L.A., Bukanov, N.O., Husson, H., Russo, R.J., Barry, T.C., Taylor, A.L., Beier, D.R. and Ibraghimov-Beskrovnaya, O. (2006) Development of polycystic kidney disease in juvenile cystic kidney mice: insights into pathogenesis, ciliary abnormalities, and common features with human disease. *J. Am. Soc. Nephrol.*, **17**, 2821–2831.
24. Sohara, E., Luo, Y., Zhang, J., Manning, D.K., Beier, D.R. and Zhou, J. (2008) Nek8 regulates the expression and localization of polycystin-1 and polycystin-2. *J. Am. Soc. Nephrol.*, **19**, 469–476.
25. Otto, E.A., Trapp, M.L., Schultheiss, U.T., Helou, J., Quarmby, L.M. and Hildebrandt, F. (2008) NEK8 mutations affect ciliary and centrosomal localization and may cause nephronophthisis. *J. Am. Soc. Nephrol.*, **19**, 587–592.
26. Shiba, D., Manning, D.K., Koga, H., Beier, D.R. and Yokoyama, T. (2010) Inv acts as a molecular anchor for Nphp3 and Nek8 in the proximal segment of primary cilia. *Cytoskeleton*, **67**, 112–119.
27. Craige, B., Tsao, C.C., Diener, D.R., Hou, Y., Lechtreck, K.F., Rosenbaum, J.L. and Witman, G.B. (2010) CEP290 tethers flagellar transition zone microtubules to the membrane and regulates flagellar protein content. *J. Cell Biol.*, **190**, 927–940.
28. Hu, Q. and Nelson, W.J. (2011) Ciliary diffusion barrier: the gatekeeper for the primary cilium compartment. *Cytoskeleton*, **68**, 313–324.
29. Omran, H. (2010) NPHP proteins: gatekeepers of the ciliary compartment. *J. Cell Biol.*, **190**, 715–717.
30. Trapp, M.L., Galtseva, A., Manning, D.K., Beier, D.R., Rosenblum, N.D. and Quarmby, L.M. (2008) Defects in ciliary localization of Nek8 is associated with cystogenesis. *Pediatr. Nephrol.*, **23**, 377–387.
31. Roig, J., Mikhailov, A., Belham, C. and Avruch, J. (2002) Nercc1, a mammalian NIMA-family kinase, binds the Ran GTPase and regulates mitotic progression. *Genes Dev.*, **16**, 1640–1658.
32. Carter, H., Samayoa, J., Hruban, R.H. and Karchin, R. (2010) Prioritization of driver mutations in pancreatic cancer using cancer-specific high-throughput annotation of somatic mutations (CHASM). *Cancer Biol. Ther.*, **10**, 582–587.
33. Corbit, K.C., Aanstad, P., Singla, V., Norman, A.R., Stainier, D.Y. and Reiter, J.F. (2005) Vertebrate Smoothened functions at the primary cilium. *Nature*, **437**, 1018–1021.
34. Schermer, B., Hopker, K., Omran, H., Ghenoiu, C., Fliegauf, M., Fekete, A., Horvath, J., Kottgen, M., Hackl, M., Zschiedrich, S. *et al.* (2005) Phosphorylation by casein kinase 2 induces PACS-1 binding of nephrocystin and targeting to cilia. *EMBO J.*, **24**, 4415–4424.
35. Deretic, D., Schmerl, S., Hargrave, P.A., Arendt, A. and McDowell, J.H. (1998) Regulation of sorting and post-Golgi trafficking of rhodopsin by its C-terminal sequence QVS(A)PA. *Proc. Natl Acad. Sci. USA*, **95**, 10620–10625.
36. Geng, L., Okuhara, D., Yu, Z., Tian, X., Cai, Y., Shibazaki, S. and Somlo, S. (2006) Polycystin-2 traffics to cilia independently of polycystin-1 by using an N-terminal RVxP motif. *J. Cell Sci.*, **119**, 1383–1395.
37. Jenkins, P.M., Hurd, T.W., Zhang, L., McEwen, D.P., Brown, R.L., Margolis, B., Verhey, K.J. and Martens, J.R. (2006) Ciliary targeting of olfactory CNG channels requires the CNGB1b subunit and the kinesin-2 motor protein, KIF17. *Curr. Biol.*, **16**, 1211–1216.
38. Mazelova, J., Astuto-Gribble, L., Inoue, H., Tam, B.M., Schonteich, E., Prekeris, R., Moritz, O.L., Randazzo, P.A. and Deretic, D. (2009) Ciliary targeting motif VxPx directs assembly of a trafficking module through Arf4. *EMBO J.*, **28**, 183–192.
39. Dishinger, J.F., Kee, H.L., Jenkins, P.M., Fan, S., Hurd, T.W., Hammond, J.W., Truong, Y.N., Margolis, B., Martens, J.R. and Verhey, K.J. (2010) Ciliary entry of the kinesin-2 motor KIF17 is regulated by importin-beta2 and RanGTP. *Nat. Cell Biol.*, **12**, 703–710.
40. Goetz, S.C. and Anderson, K.V. (2010) The primary cilium: a signalling centre during vertebrate development. *Nat. Rev. Genet.*, **11**, 331–344.

41. Wong, S.Y. and Reiter, J.F. (2008) The primary cilium at the crossroads of mammalian hedgehog signaling. *Curr. Top. Dev. Biol.*, **85**, 225–260.
42. Natoli, T.A., Gareski, T.C., Dackowski, W.R., Smith, L., Bukanov, N.O., Russo, R.J., Husson, H., Matthews, D., Piepenhagen, P. and Ibraghimov-Beskrovnaya, O. (2008) Pkd1 and Nek8 mutations affect cell-cell adhesion and cilia in cysts formed in kidney organ cultures. *Am. J. Physiol. Renal Physiol.*, **294**, F73–F83.
43. Yim, H., Sung, C.K., You, J., Tian, Y. and Benjamin, T. (2011) Nek1 and TAZ interact to maintain normal levels of polycystin 2. *J. Am. Soc. Nephrol.*, **22**, 832–837.
44. Bowers, A.J. and Boylan, J.F. (2004) Nek8, a NIMA family kinase member, is overexpressed in primary human breast tumors. *Gene*, **328**, 135–142.
45. Han, Y.G., Kim, H.J., Dlugosz, A.A., Ellison, D.W., Gilbertson, R.J. and Alvarez-Buylla, A. (2009) Dual and opposing roles of primary cilia in medulloblastoma development. *Nat. Med.*, **15**, 1062–1065.
46. Wong, S.Y., Seol, A.D., So, P.L., Ermilov, A.N., Bichakjian, C.K., Epstein, E.H. Jr, Dlugosz, A.A. and Reiter, J.F. (2009) Primary cilia can both mediate and suppress Hedgehog pathway-dependent tumorigenesis. *Nat. Med.*, **15**, 1055–1061.
47. Hildebrandt, F. and Otto, E. (2005) Cilia and centrosomes: a unifying pathogenic concept for cystic kidney disease? *Nat. Rev. Genet.*, **6**, 928–940.
48. Pazour, G.J. (2004) Intraflagellar transport and cilia-dependent renal disease: the ciliary hypothesis of polycystic kidney disease. *J. Am. Soc. Nephrol.*, **15**, 2528–2536.
49. Fischer, E., Legue, E., Doyen, A., Nato, F., Nicolas, J.F., Torres, V., Yaniv, M. and Pontoglio, M. (2006) Defective planar cell polarity in polycystic kidney disease. *Nat. Genet.*, **38**, 21–23.
50. Nishio, S., Tian, X., Gallagher, A.R., Yu, Z., Patel, V., Igarashi, P. and Somlo, S. (2010) Loss of oriented cell division does not initiate cyst formation. *J. Am. Soc. Nephrol.*, **21**, 295–302.
51. Zhang, J., Wu, M., Wang, S., Shah, J.V., Wilson, P.D. and Zhou, J. (2010) Polycystic kidney disease protein fibrocystin localizes to the mitotic spindle and regulates spindle bipolarity. *Hum Mol. Genet.*, **19**, 3306–3319.
52. Chen, Y., Chen, C.F., Riley, D.J. and Chen, P.L. (2011) Nek1 kinase functions in DNA damage response and checkpoint control through a pathway independent of ATM and ATR. *Cell Cycle*, **10**, 655–663.
53. Hames, R.S. and Fry, A.M. (2002) Alternative splice variants of the human centrosome kinase Nek2 exhibit distinct patterns of expression in mitosis. *Biochem. J.*, **361**, 77–85.
54. Fry, A.M., Mayor, T., Meraldi, P., Stierhof, Y.D., Tanaka, K. and Nigg, E.A. (1998) C-Nap1, a novel centrosomal coiled-coil protein and candidate substrate of the cell cycle-regulated protein kinase Nek2. *J. Cell Biol.*, **141**, 1563–1574.
55. Hames, R.S., Crookes, R.E., Straatman, K.R., Merdes, A., Hayes, M.J., Faragher, A.J. and Fry, A.M. (2005) Dynamic recruitment of Nek2 kinase to the centrosome involves microtubules, PCM-1, and localized proteasomal degradation. *Mol. Biol. Cell*, **16**, 1711–1724.